


---

This is the **accepted version** of the journal article:

Cueto, David; Mora Garrido, Mabel; Gabriel, David. «Evaluating and modeling biological sulfur production in the treatment of sulfide-laden streams containing ammonium». *Journal of chemical technology and biotechnology*, Vol. 96, Issue 2 (February 2021), p. 439-447. DOI 10.1002/jctb.6558

---

This version is available at <https://ddd.uab.cat/record/266995>

under the terms of the  <sup>IN</sup> COPYRIGHT license

# Evaluating and modeling the biological sulfur production in the treatment of sulfide-laden streams containing ammonium

David Cueto<sup>1</sup>, Mabel Mora<sup>1</sup>, David Gabriel<sup>1\*</sup>.

<sup>1</sup>GENOCOV Research Group, Department of Chemical, Biological and Environmental Engineering, Escola d'Enginyeria, Universitat Autònoma de Barcelona, 08193 Bellaterra, Spain.

Corresponding author: (david.gabriel@uab.cat).

## ABSTRACT

### Background

Biological treatment of effluents containing H<sub>2</sub>S and ammonium are of great interest as both compounds can trigger serious environmental problems when disposed of. The aim of this study was to optimize the production of biosulfur from the partial oxidation of sulfide in sulfide- and ammonium-containing streams. Biological performance was evaluated under different aerating conditions and key kinetic parameters were adjusted based on an existing mathematical model adapted to this system.

### Results

An optimal conversion of sulfide to S<sup>0</sup> of 86 % (w/w) was found at an oxidation-reduction potential (ORP) of  $-380 \pm 10$  mV and at an O<sub>2</sub>/S<sup>2-</sup> molar ratio of 0.44. Partial nitrification was observed at ORP higher than -200 mV and in excess of oxygen supply. Sulfide-oxidizing bacteria (SOB) outcompeted ammonium-oxidizing bacteria (AOB) in the competition for dissolved oxygen. In a modelling effort, the maximum specific growth rate for SOB, the sulfur shrinking kinetic constant, the maximum specific growth rate for AOB and the AOB oxygen half saturation constants were adjusted to 10.1 d<sup>-1</sup>, 0.3 mg<sup>2/3</sup> VSS mg<sup>-2/3</sup> S, 1.75 d<sup>-1</sup> and 1.5 mg L<sup>-1</sup>, respectively, during model calibration.

### Conclusions

Optimal S<sup>0</sup> production was found under limiting O<sub>2</sub> conditions in which AOB were not able to outcompete SOB. The mathematical model described satisfactorily the experimental profiles for ammonium, nitrite, sulfide and sulfate as a function of the aeration flowrate.

1 **Keywords:** sulfide; oxygen competition; biological sulfur production; partial nitrification;  
2 mathematical model

### 3 **1. Introduction**

4 Sulfate-rich streams generated in pulp and paper factories, food industry, tannery industry,<sup>1</sup>  
5 oil extraction and mining activities amongst others are ideal for sulfate reducing bacteria  
6 (SRB) growth under anaerobic conditions, which produces sour effluents with high sulfide  
7 content. H<sub>2</sub>S is the most concerning S-compound because of its toxicity, low odor threshold  
8 and its potential as precursor of SO<sub>x</sub> gases when combusted.<sup>2</sup> Also, sulfide-laden streams  
9 cause corrosion of pipelines<sup>3</sup> and plugging<sup>4</sup> when sulfide is completely or partially oxidized,  
10 respectively. Some sulfide-rich streams may also contain significant concentrations of  
11 ammonium. This is the case of those effluents generated in anaerobic reactors treating sulfate  
12 and nitrogen containing wastewater, such as tannery wastewater<sup>5</sup> and the two-step  
13 bioscrubbing process for the recovery of elemental sulfur (S<sup>0</sup>) from combustion gases  
14 containing SO<sub>x</sub>.<sup>6</sup> Valorization of sulfur from sulfur dioxide (SO<sub>2</sub>) has important advantages  
15 as SO<sub>2</sub> is a contaminant with worldwide emissions for 2010 estimated to be  $6 \times 10^7$  S-SO<sub>2</sub>  
16 tones,<sup>7</sup> that causes acid rains and formation of sulfate aerosols that affect solar radiation.<sup>8</sup>  
17 Additionally, SO<sub>2</sub> recovered as S<sup>0</sup> can be reused in sectors such as agriculture,<sup>9</sup> Li-S  
18 batteries<sup>10</sup> and S-based pigments production.<sup>11,12</sup> The reintegration of contaminants into the  
19 economy as valorized products is the main principle of a circular economy, an essential step  
20 for sustainability in which treatment of residues is aimed at diminishing environmental  
21 impacts and economical expenses.<sup>13</sup>

22

23 The biological production, recovery and valorization of elemental sulfur demand an  
24 optimization, not only of the biological process but also of the downstream stages, such as  
25 precipitation and purification, to enhance the overall process productivity. The biological  
26 sulfur production is mainly governed by operational parameters like dissolved oxygen (DO)  
27 and sulfide concentrations, which have major impacts on the oxidation-reduction potential  
28 (ORP). The latter has been reported as the key variable to control S<sup>0</sup> formation.<sup>14</sup> In a  
29 biotechnological process treating sulfide- and ammonium-containing effluents, operational  
30 parameters such as DO, stirring rate, hydraulic residence time (HRT), pH and temperature  
31 will affect the kinetics and, consequently, the proliferation of different microorganisms that

1 will compete for oxygen. Biological sulfide oxidation can be partial or complete (equations  
 2 1 and 2) depending on the O<sub>2</sub> and HS<sup>-</sup> molar ratio. Similarly, ammonium oxidation will be  
 3 governed by the O<sub>2</sub> and NH<sub>4</sub><sup>+</sup> molar ratio (equations 3 to 5). Biological ammonium oxidation  
 4 implies the production of NH<sub>2</sub>OH as an intermediate that, due to its high reactivity,<sup>15</sup> it is  
 5 barely accumulated. Consequently, NH<sub>2</sub>OH is not normally considered in the nitrification  
 6 process.<sup>16</sup> However, under certain conditions NH<sub>2</sub>OH is a precursor for the formation of N<sub>2</sub>O  
 7 (Eq. 6), which may be significant depending on process conditions. Finally, chemical  
 8 precipitation of (NH<sub>4</sub>)<sub>2</sub>SO<sub>4</sub> (Eq. 7) can take place if ammonium and sulfate concentrations  
 9 are high enough to reach its solubility product, often difficult for diluted effluents due to its  
 10 high solubility (790 g (NH<sub>4</sub>)<sub>2</sub>SO<sub>4</sub> per liter of water).<sup>17</sup> Moreover, its production is enhanced  
 11 at temperatures over 60°C and acidic conditions (pH below 3).<sup>18</sup>

12



13

14 Consumption and production rates can be described by kinetic equations together with mass  
 15 balances already reported in the literature. Regarding ammonium-oxidizing bacteria (AOB)  
 16 and nitrite-oxidizing bacteria (NOB), different experimental works and mathematical models  
 17 have been proposed in the literature to describe AOB/NOB activity. Well-established models  
 18 exist to describe the nitrification process,<sup>19</sup> and lots of previous works have modeled the  
 19 nitrification process based on Monod-type models to estimate kinetic parameters.<sup>20</sup> In  
 20 comparison, literature regarding mathematical modelling of SOB activity is more limited.  
 21 Amongst others, Roosta *et al.*<sup>21</sup> described a fed-batch bioreactor using a mathematical model  
 22 to understand the effect of sulfide load in the system. On the other hand, Mora *et al.*<sup>22</sup> reported  
 23 a two-step sulfide-oxidation model that considered the strong effect of sulfide inhibition

1 using a Haldane-type equation coupled with a shrinking particle constant to describe the  
2 intracellular sulfur accumulation for a *Thiotrix spp.* SOB culture. However, to the authors  
3 knowledge, the competition among them in a bioreactor treating together sulfide- and  
4 ammonium-loaded wastewater has not been previously reported.

5  
6 This work targets the production of biosulfur from the partial oxidation of sulfide in sulfide-  
7 and ammonium-containing streams. To this aim, this work evaluated the performance of a  
8 biological culture under different aeration conditions to promote biosulfur production and to  
9 study the microbial competition for the electron acceptor both from an experimental and a  
10 mathematical modelling approach.

## 11 12 **2. Materials and Methods**

### 13 *2.1 Experimental setup and operating conditions*

14 In this study the experimental assays lasted for 62 days and were performed in a 3L lab-scale  
15 biostat that was inoculated with a mixed culture obtained from a full-scale THIOPAQ™  
16 process installed in a pulp and paper industry. This THIOPAQ™ process was fed with  
17 ammonium as nutrient and aims to treat high sulfide load wastewaters, being a niche for the  
18 growth of sulfide oxidizing and nitrifying microorganisms; that explains the high sulfide and  
19 ammonium oxidation activity from the beginning of the experiment (see section 3.1). The  
20 experimental setup is shown in Fig. 1. Mineral medium (MM) was fed at a flow rate of  $110$   
21  $\pm 7$  mL h<sup>-1</sup> and a sodium sulfide stock solution of  $5$  g L<sup>-1</sup> was prepared and fed at a flow rate  
22 of  $15$  mL h<sup>-1</sup>, which resulted in an equivalent inlet total dissolved sulfide (TDS) concentration  
23 of  $600 \pm 50$  mg S L<sup>-1</sup>, a volumetric load of  $24 \pm 3$  mg S L<sup>-1</sup> h<sup>-1</sup> and a hydraulic residence time  
24 (HRT) of 25h. The MM composition was as follows (in g L<sup>-1</sup>): NaHCO<sub>3</sub> (3.89), NH<sub>4</sub>Cl (1.1),  
25 KH<sub>2</sub>PO<sub>4</sub> (0.13), K<sub>2</sub>HPO<sub>4</sub> (0.17), CaCl<sub>2</sub> (0.02), MgSO<sub>4</sub>·7H<sub>2</sub>O (0.22) and trace element  
26 solution (1 ml L<sup>-1</sup>). MM and sulfide were fed separately with peristaltic pumps to avoid  
27 sulfide salts precipitation. A CO<sub>2</sub> flow of  $50$  mL min<sup>-1</sup> was mixed with an inlet air flow to  
28 supply the carbon source and the oxygen needed for the autotrophic mixed culture. CO<sub>2</sub> and  
29 air were supplied, measured and controlled with mass flow controllers (Bronckhorst, The  
30 Netherlands).

1 The experiment was divided in 7 periods that were defined by different air flow rates (Table  
2 1) to study the biological competition of SOB and nitrifiers for O<sub>2</sub> and the S<sup>0</sup> production.  
3 Temperature, pH, DO and ORP in the biostat were monitored on-line. A home-made software  
4 developed in Visual Basic was used for data acquisition and control. The pH was controlled  
5 between 7.4-7.6 by an on/off controller adding NaOH (2M) and HCl (2M) solutions. As the  
6 case under study was the two-step bioscrubbing process for biosulfur recovery from SO<sub>2</sub>, a  
7 thermostatic water bath was used to control the biostat temperature at 33°C according to  
8 process conditions reported by Fernández *et al.*<sup>6</sup> It is worth mentioning that the optimal  
9 temperature for chemolithotrophic SOB is between 28 and 35°C,<sup>2</sup> and AOB activity is favored  
10 at temperatures above 30°C according to a SHARON process,<sup>23</sup> which means that SOB and  
11 AOB growth is enhanced at 33°C. The stirring was kept at 230 rpm along the experiment.  
12 Since stirring also contributes to oxygen supply, a flat blade turbine type stirrer was used  
13 (IKA RW 20 digital). The biostat was cleaned periodically to avoid biofilm accumulation on  
14 its walls and stirrer and an activated carbon filter was used to avoid hydrogen sulfide release  
15 in air.

16  
17 In addition, a set of abiotic experiments were performed to determine the total oxygen  
18 supplied in each of the seven periods using the dynamic gas in-gas out method.<sup>24</sup> The  
19 volumetric mass transfer coefficient was calculated from a mass balance model according to  
20 the standardized ASCE/EWRI 2-06 equation under dynamic conditions.<sup>25</sup> The mass transfer  
21 coefficient estimation is explained in detail in the Supporting Information (Section 1).

22  
23 Table 1 shows the oxygen mass transfer coefficients ( $K_{La}$ ), the oxygen-sulfide and oxygen-  
24 ammonium molar ratios of each period. The start-up of the biostat lasted 4 days keeping the  
25 oxygen supply in excess by setting an air flow rate of 0.8 L min<sup>-1</sup> (data not shown).

## 26 27 *2.2 Analytical methods*

28 TDS was measured off-line by an ion-selective electrode (VWR International Eurolab, S.L.)  
29 connected to a bench-top meter (Symphony, VWR, USA). This electrode has a high  
30 sensitivity to the completely dissociated form of sulfide (S<sup>2-</sup>), which made necessary to  
31 prepare the samples in an alkaline antioxidant buffer solution (SAOB) before measurement.<sup>22</sup>

1 Ammonium concentration in the MM and in the biostat was measured off-line with an  
2 ammonium analyzer (AMTAX sc, Hach Lange, Germany). The concentration of oxidized  
3 sulfur and nitrogen species ( $\text{SO}_4^{2-}$ ,  $\text{SO}_3^{2-}$ ,  $\text{S}_2\text{O}_3^{2-}$ ,  $\text{NO}_3^-$  and  $\text{NO}_2^-$ ) were measured by ion  
4 chromatography (Dionex ICS-2000 HPLC system, Dionex, USA). Sulfite was not detected  
5 along the biostat operation and subsequently was not considered for the sulfur mass balance.  
6 The ion chromatography equipment has a suppressed conductivity detector and uses an  
7 IonPac AS18-HC column (4X250 mm – Dionex, USA). Prior to the analysis, samples were  
8 filtered with a 0.22  $\mu\text{m}$  cellulose filter and bubbled with nitrogen to avoid changes in  
9 concentration due to chemical oxidation of  $\text{H}_2\text{S}$ .

10  
11 DNA extraction of suspended biomass in the biostat was performed when the reactor was  
12 aerated with 0.35 L air  $\text{min}^{-1}$  (day 15 of operation) to analyze the microbial diversity grown  
13 in the biostat. The MoBio PowerBiofilm<sup>TM</sup> DNA extraction kit (MoBio Laboratories, USA)  
14 protocol was applied with two modifications in the extraction process as it was described by  
15 Reino *et al.*<sup>26</sup> The quality and quantity of the extracted DNA was measured using NanoDrop  
16 1000 Spectrophotometer (Thermo Fisher Scientific, USA). Illumina sequencing of the DNA  
17 was performed using the primers Bakt-515F (5' GTG CCA GCM GCC GCG GTA A') and  
18 Bakt\_909R (5' CCG TCA ATT YHT TTR AGT 3') with a minimum DNA concentration of  
19 20 ng  $\text{L}^{-1}$  using the Illumina MiSeq platform (AllGenetics, A Coruña, Spain).

20  
21 Elementary analysis was also performed during the last period when the elemental sulfur  
22 production was the highest and steady. The sample was centrifuged at 12000 rpm (Micro  
23 Centrifuge Model 16K, BioRAD, USA), lyophilized for 8 hours (Sentry 12525, The VirTis  
24 Company, New York) and stored at  $-25^\circ\text{C}$  to avoid chemical oxidation of sulfur. Then,  
25 carbon, hydrogen, nitrogen and sulfur contained in the solid were analyzed by combusting  
26 the sample in an oxygen atmosphere at  $1200^\circ\text{C}$  and analyzing the produced gas by gas  
27 chromatography (Elemental Analyzer CHNS Thermo Scientific Flash 2000).

### 28 29 *2.3 Mathematical model*

30 The mathematical model is represented in Table SI3 following Peterson Matrix  
31 representation.<sup>27</sup> The set of kinetic equations used to describe SOB growth was partly

1 selected from the model proposed by Mora *et al.*<sup>22</sup> However, in the present study the  
2 intracellular  $S^0$  accumulation term was not considered (see Table SI4) since the microbial  
3 analysis revealed the absence of intracellular  $S^0$  accumulating SOB (see section 3.3). The set  
4 of kinetic and differential equations used in this study are shown in the Supporting  
5 Information (section 3).

6  
7 The mathematical model was programmed in MATLAB R2013b. The set of differential  
8 equations was solved using the MATAB ODE15s function. A sensitivity analysis was  
9 performed to determine the most sensible kinetic parameters over an objective function ( $f_{obj}$ )  
10 defined as the norm of the difference between experimental and the mathematical model data  
11 for sulfide, sulfate, nitrite and DO (Eq. SI3).<sup>22</sup> This analysis was performed by changing by  
12  $\pm 10\%$  one at a time each kinetic parameter of the model and evaluating the objective function.  
13 The relative standard deviation (RSD) of the function was determined to identify the  
14 sensitivity. Afterwards, the model was calibrated using the *fminsearch* function in Matlab  
15 and using experimental data of the 6 first periods of operation of the reactor (Table 1). This  
16 fitting method minimizes the  $f_{obj}$  by adjusting the most sensible kinetic parameters, those  
17 determined from the sensitivity analysis, to fit model predictions to experimental data. Data  
18 from the last experimental period (after day 37) conducted under different experimental  
19 conditions than those along the calibration stage were used to validate the model.

20  
21 Results obtained from the mathematical model fitting to the experimental data were  
22 statistically evaluated by using a two-tailed t-student distribution of independent samples.  
23 The evaluation consisted of the comparison between mean values of two data sets and the  
24 determination of a t-value and a p-value calculated using Eq. SI4 (Supporting Information)  
25 and standard t-tables, respectively.<sup>28</sup>

## 26 27 **3. Results and discussion**

### 28 *3.1 Biological sulfur production and oxygen competition by sulfide oxidizing and nitrifying* 29 *microorganisms*

30 The biological sulfide and ammonium oxidation were analyzed along the operation of the  
31 biostat according to the operating periods shown in Table 1. Figure 2 shows the sulfur mass



1 balance along the experiment (Fig. 2A) and the concentration of the main sulfur (Fig. 2B)  
2 and nitrogen (Fig. 2C) species as an average concentration measured in each operating period  
3 (Table 1) once the steady-state was reached. The  $S^0$  production per hour was determined by  
4 mass balance as the difference between the total sulfur species in the inlet and outlet (see  
5 section 2 of Supporting Information), a calculation that has been already reported in other  
6 works.<sup>29,30</sup>

7  
8 Sulfur species mass flowrates in Fig. 2A corresponded to an inlet TDS of  $89 \pm 3$  % (w/w) plus  
9 a  $4 \pm 3$  % (w/w) of sulfate and  $6 \pm 1$  % (w/w) of thiosulfate of the total S-species in the inlet.  
10 From day 0 to 17 the air flowrate was stepwise reduced from  $1 \text{ L min}^{-1}$  to  $0.35 \text{ L min}^{-1}$  (Table  
11 1). The oxidation of  $HS^-$  to  $SO_4^{2-}$  was 99 % as expected based on the  $O_2$ /TDS molar ratio,  
12 which was in excess with respect to the stoichiometric oxygen required to oxidize 1 mol of  
13  $S^{2-}$  to  $S^0$  (Eq. 1). Due to the low cleaning frequency of the biostat, that was initially performed  
14 every 10 days, the partial accumulation of  $S^0$  over the walls and stirrer resulted in a higher  
15 net sulfur quantity in the outlet since the accumulated  $S^0$  was further oxidized to sulfate. This  
16 explains the sulfur imbalance observed along the first 23 days of operation.

17  
18 From day 19 to 24, the oxidation of sulfide to sulfate decreased to 62.3 % (w/w) at an air  
19 flow rate of  $0.2 \text{ L min}^{-1}$ . From day 24 to 37, the oxidation of sulfide to sulfate decreased  
20 down to 54.3 % (w/w) at an air flow rate of  $0.05 \text{ L min}^{-1}$  and an  $O_2/HS^-$  molar ratio of 1.5  
21 (Table 1), which was lower than the stoichiometric oxygen required for a complete sulfide  
22 oxidation ( Eq. 1 and 2). After day 37, the air flow was stopped, and oxygen was only  
23 supplied by stirring. The  $O_2/HS^-$  molar ratio supplied was 0.44, while the stoichiometric value  
24 for the partial oxidation to  $S^0$  is 0.5 according to equation 1. As it can be seen in Figure 2A,  
25 the elemental sulfur production started to increase. On day 42, a sulfide load shock of  $1200$   
26  $\text{mg S-S}^{2-} \text{ L}^{-1}$  was applied and the process kept the partial oxidation of sulfide to  $S^0$  over 75  
27 % (w/w), reaching an 86 % (w/w) conversion to  $S^0$  in the last days of this period. Other works  
28 have reported that  $O_2/HS^-$  molar ratios between 0.6 and 1 are needed to enhance  $S^0$   
29 production<sup>31,32</sup> while for ratios lower than 0.6, thiosulfate is the predominant product.<sup>33</sup> The  
30 lower molar ratio of 0.44 reported here imply a higher efficiency in terms of oxygen  
31 consumption at such a high sulfide conversion to  $S^0$ .

1

2 Analyzing the S-species based on the steady-state concentrations achieved during each  
3 period (Fig. 2B), the complete sulfide oxidation started to decrease progressively when the  
4 air flow rate was reduced from 0.35 to 0.2 L min<sup>-1</sup> (Fig. 2B). The latter corresponded to an  
5 O<sub>2</sub>/TDS molar ratio of 2.9, which was higher than 2, the stoichiometric molar ratio needed  
6 for a complete sulfide oxidation (Eq. 1 and 2), thus indicating that other aerobic species were  
7 competing with sulfide-oxidizing bacteria for O<sub>2</sub>.

8 Regarding nitrogen species profiles in Figure 2C, AOB activity was observed until period  
9 IV, indicating that under those conditions, oxygen competition between AOB and SOB was  
10 taking place. Moreover, nitrate was not observed along the biostat operation (Fig. 2C). The  
11 lack of nitrate could be related with the kinetics of NOB. NOB and AOB have been reported  
12 to have a duplication time of 50h and 17h at 25°C, respectively,<sup>20</sup> and the HRT of the biostat  
13 was set at 25h which was lower than the NOB duplication time. The accumulation of NOB  
14 in the biofilm was avoided by a periodical cleaning of the biostat wall; meanwhile AOB did  
15 not have a microbial growth limitation since the growth rate was higher than the dilution rate.  
16

17 Moreover, a nitrogen mass balance was performed (Figure SI3). NO formation was not  
18 considered as its production relies on low pH conditions.<sup>15</sup> Since (NH<sub>4</sub>)<sub>2</sub>SO<sub>4</sub> formation is  
19 favored at pH below 3, temperature over 60°C<sup>18</sup> and is highly soluble, its precipitation was  
20 not considered in the mass balance. Nitrogen uptake for biomass growth was estimated based  
21 on the biomass production estimated by the mathematical model (section 3.3) and the  
22 nitrogen content of the elemental composition of biomass, which is 6.1% (w/w) for sewage  
23 sludge.<sup>34</sup> Consequently, the nitrogen imbalance of 18 ± 9 mg N L<sup>-1</sup> along the experimental  
24 periods could be due to a nitrous oxide (N<sub>2</sub>O) formation as it has been reported in processes  
25 with nitrifying bacteria.<sup>9,35,36</sup>

26

27 Analyzing the conversion of ammonium to nitrite, all ammonium was oxidized when the air  
28 flow rate was 1 L min<sup>-1</sup>. After that, ammonium oxidation decreased progressively along the  
29 following periods and nitrite was not further detected when air flow rate was 0.2 L min<sup>-1</sup>.  
30 Under this condition, the DO/N-NH<sub>4</sub><sup>+</sup> and DO/TDS molar ratios were 3.2 and 2.9 (Table 1),  
31 respectively. These ratios are higher than the stoichiometric oxygen requirements for

1 ammonium and sulfide oxidation (Eq. 1 to 5) even if such oxygen consumption reduced the  
2 DO to below  $1 \text{ mg L}^{-1}$ , period V of Figure 3. Guisasola *et al.*<sup>16</sup> reported an oxygen half  
3 saturation constant for AOB of  $0.74 \text{ mg L}^{-1}$  while Mora *et al.*<sup>22</sup> reported a value of  $0.15 \text{ mg}$   
4  $\text{L}^{-1}$  for SOB. Consequently, the decrease in the AOB activity was attributed to the higher  
5 oxygen affinity by SOB, which means that under limiting oxygen environment, SOB  
6 outcompetes AOB.

7  
8 Moreover, AOB are highly sensitive to low sulfide concentrations. The  $\text{IC}_{50}$  for AOB  
9 reported in literature ranges from  $3 \pm 0.3 \text{ mg TDS L}^{-1}$ ,<sup>37</sup> to  $0.7 \text{ mg TDS L}^{-1}$ .<sup>38</sup> Since sulfide  
10 concentrations were around  $1 \text{ mg L}^{-1}$  in the reactor during the first 40 days, partial inhibition  
11 of AOB by free sulfide could have occurred in this stage. This inhibition effect was also  
12 studied by Sekine *et al.*<sup>39</sup> who implemented a sequential batch reactor with a HRT of 3 days  
13 and a solid retention time of 170 days to evaluate the biological oxidation of ammonium and  
14 sulfide. In that case, nitrification was not affected at inlet sulfide loads lower than  $5.3 \text{ mg S}$   
15  $\text{L}^{-1} \text{ h}^{-1}$  while ammonium removal efficiency decreased from 100 to 50 % at inlet sulfide loads  
16 of  $10.7 \text{ mg S L}^{-1} \text{ h}^{-1}$ . In the present work, a sulfide load of  $24 \text{ mg S L}^{-1} \text{ h}^{-1}$  (see Section 2.1)  
17 and the major oxygen affinity by SOB could explain the rapid decrease of AOB activity. It  
18 is worth mentioning that Jiang *et al.*<sup>40</sup> reported ammonium removal efficiencies over 95 %  
19 for sulfide loads of  $164 \text{ mg L h}^{-1}$ ; however, results were found in a biostat for simultaneous  
20 biological treatment of ammonium and sulfide with 17 days of acclimatization period.  
21 Further studies of acclimatization periods are warranted to couple ammonium treatment and  
22 biosulfur production.

23  
24 To analyze the optimal conditions that enhance the production of nitrite and elemental sulfur,  
25 and considering that ORP and DO have been reported as key parameters to control the  
26 biological sulfide oxidation,<sup>9</sup> the ORP, DO and  $\text{S}^0$  are depicted in Figure 3. It can be observed  
27 that in the last period (Fig. 3), when air flow rate was  $0 \text{ L min}^{-1}$  (Table 1), the ORP reached  
28 the most negative value while DO reached its lowest concentration. This occurred because  
29 the decrease in oxygen shifts the medium from an oxidative to a reductive environment.  
30 Based on the partial nitrification previously analyzed and results from Figure 3, no AOB  
31 activity was observed when ORP was less than  $-200 \text{ mV}$ . Meanwhile, the optimal ORP for

1 sulfur production was found to be  $-380 \pm 10$  mV with a  $S^0$  concentration of  $594 \text{ mg L}^{-1}$ , a  
2 sulfide to  $S^0$  conversion of 86 % (w/w) and a TDS accumulation in the reactor of  $30 \text{ mg L}^{-1}$ ,  
3 equivalent to 5 % (w/w) of the inlet sulfide. This conversion was obtained for a TDS/N-NH<sub>4</sub><sup>+</sup>  
4 molar ratio of 1.2 and an O<sub>2</sub>/TDS of 0.44 (Table 1). Similar values have been reported in the  
5 literature for partial sulfide oxidation process under non O<sub>2</sub>-competition with SOB/AOB by  
6 Krishnakumar *et al.*,<sup>41</sup> who implemented a reverse fluidized loop reactor for  $S^0$  recovery; a  
7 97 % (w/w) sulfide removal, 3 % (w/w) sulfide accumulation and 80 % (w/w) sulfur recovery  
8 under an ORP between -400 and -350 mV were reported. Similarly, Vannini *et al.*<sup>42</sup> used a  
9 membrane reactor for biological sulfur production and found an optimal ORP between -400  
10 and -360 mV obtaining a sulfide conversion to  $S^0$  of 79 % (w/w).

11

### 12 3.2 Microbial diversity characterization

13 Fig. 4 shows the results obtained from the microbial diversity analysis. The sample was taken  
14 from the suspended biomass on day 15 of operation, when air flow rate was  $0.35 \text{ L min}^{-1}$ .  
15 Halothiobacillaceae was the most abundant sulfide oxidizing family with a relative  
16 abundance of 45 % in the suspended biomass (Fig. 4); the high salt content in the mineral  
17 medium (see section 2.1) could also explain the large quantity of halotolerant  
18 microorganisms grown in the biostat. Betaproteobacteria class represented 25 % of the  
19 culture abundance (accounted in Fig. 4 in the unclassified group), which means that some  
20 other sulfide oxidizing microorganisms belonging to this class could be present in the culture  
21 medium such as *Thiobacillus* genera. Some other SOB species could have been also present  
22 in the biostat since 1 % and 9 % of the suspended culture were identified as Comamonadaceae  
23 and Xanthomonadaceae families (see Fig. 4), respectively. In fact, *Delftia*<sup>43</sup> and  
24 *Rhodanobacter* have been reported as SOB that belong to the abovementioned families,  
25 respectively.<sup>44</sup>

26

27 Regarding the nitrifying microbial diversity, 1.6 % of the suspended culture were AOB  
28 belonging to the Nitrosomonadaceae family (Fig. 4), which was probably highly active since  
29 the NH<sub>4</sub><sup>+</sup> oxidation in this period ( $0.35 \text{ L air min}^{-1}$ ) was 55 % (w/w) (Fig. 2C) for an  
30 ammonium load of  $9.3 \pm 0.3 \text{ mg N-NH}_4^+ \text{ L}^{-1} \text{ h}^{-1}$ . NOB-type families were not identified in  
31 the suspended culture which is consistent with the fact that only partial nitrification

1 (nitrification) was observed. Additionally, as no autotrophic denitrifiers such as *Thiobacillus*  
2 *denitrificans* were found and oxygen was in excess during the first 5 periods, it is unlikely  
3 that denitrification took place; . based on this, denitrification process was not considered for  
4 the mathematical modeling.

### 6 3.3 Modeling SOB and nitrifying activity

7 Mass balances, stoichiometric and kinetic equations were used to describe the performance  
8 of the biostat and to further assess the competition between SOB and nitrifying species for  
9 DO, which has not been reported previously to the authors knowledge. Existing models  
10 describing nitrifying (ASM models) and SOB activity<sup>22</sup> were used. However, significant  
11 changes were made to the model reported by Mora *et al.*<sup>22</sup> for sulfide oxidation. The latter  
12 considered that elemental sulfur was accumulated inside the cells during the partial oxidation  
13 of sulfide since the culture was mainly composed by *Thiobacillus* spp (>95%). In our work,  
14 Illumina sequencing results did not show any SOB of the family Thiobacillaceae, which are  
15 the ones reported to accumulate intracellular S<sup>0</sup>.<sup>2</sup> Therefore, model equations used to describe  
16 the kinetics of sulfide oxidation in the present work (see section 3, Supporting Information)  
17 were adapted accordingly. Thus, a Haldane-type kinetic equation was used to describe sulfide  
18 oxidation by SOB.

19  
20 In order to understand the sulfide conversion to sulfate/sulfur and the competition with AOB,  
21 a sensitivity analysis was performed. The kinetic parameters  $\mu_{\max/\text{SOB}}$ ,  $k_{\text{S}^0}$ ,  $\mu_{\max/\text{AOB}}$  and  
22  $k_{\text{O}_2/\text{AOB}}$  were the most sensitive parameters in this system (see Table SI7, Supporting  
23 Information). Consequently, these parameters were chosen to calibrate the model while all  
24 other parameters were kept as those reported in literature (see Table SI2, Supporting  
25 Information). Table 2 shows the parameters obtained after model calibration while Figure 5  
26 shows model predictions of the whole experimental period, thus including the validation  
27 period after day 38. Remarkably, only 4 parameters out of 21 kinetic parameters were enough  
28 to satisfactorily model the experimental data for S and N species and DO in Figure 5,  
29 corroborating the high sensitivity of these parameters. Parameters calibrated were in the  
30 range of previously reported values; the latter are shown in Table 3. Munz *et al.*<sup>45</sup> reported a  
31  $\mu_{\max/\text{SOB}}$  of 7.4 d<sup>-1</sup> (25°C) for a predominant culture of Halothiobacillaceae family in a

1 membrane reactor working with a solid retention time (SRT) of 5 days. Mora *et al.*<sup>22</sup> obtained  
2 a  $\mu_{\max/\text{SOB}}$  of  $9.84 \text{ d}^{-1}$  ( $25^\circ\text{C}$ ) from respirometric experiments for a predominant culture of  
3 *Thriotrix* genus in a biostat with 2.8 days of SRT. Likewise, Mora *et al.*<sup>22</sup> reported values for  
4  $k_{\text{S}^0}$  in the range of 0.833 and 0.03 ( $25^\circ\text{C}$ ), similar to the results obtained from the model  
5 calibration performed in this work. In the case of  $\mu_{\max/\text{AOB}}$ , Wu *et al.*<sup>20</sup> and Jubany *et al.*<sup>46</sup>  
6 reported values of  $1.45 \text{ d}^{-1}$  and  $1.21 \text{ d}^{-1}$  ( $25^\circ\text{C}$ ), respectively; in this work, a higher value of  
7  $1.75 \text{ d}^{-1}$  (Table 2) was achieved. Even though, the calibration resulted in a higher oxygen  
8 affinity constant for AOB ( $k_{\text{O}_2/\text{AOB}} = 1.5 \text{ d}^{-1}$ ) compared to those reported in the literature; this  
9 could explain the AOB depletion under oxygen limitation. Pan *et al.*<sup>47</sup> obtained a  $k_{\text{O}_2/\text{AOB}}$  of  
10  $0.6 \text{ mg L}^{-1}$  ( $22^\circ\text{C}$ ). Ge *et al.*<sup>48</sup> studied the partial nitrification in wastewater treatment plants  
11 and found that  $k_{\text{O}_2/\text{AOB}}$  was between 0.22 and  $0.56 \text{ mg L}^{-1}$  ( $25^\circ\text{C}$ ) for straight rods-type  
12 *Nitrosomonas*, while Guisasola *et al.*<sup>16</sup> found it to be  $0.74 \text{ mg L}^{-1}$  ( $25^\circ\text{C}$ ). A value closer to  
13 the  $k_{\text{O}_2/\text{AOB}}$  found in this work was reported by Regmi *et al.*<sup>49</sup> with a  $k_{\text{O}_2/\text{AOB}}$  of  $1.16 \text{ mg L}^{-1}$   
14 ( $25^\circ\text{C}$ ) for a suspended culture.

15

16 In Figure 5A, model and experimental data profiles corresponding to the three main sulfur  
17 species – TDS,  $\text{S}^0$  and sulfate – are depicted. It can be observed that sulfate profiles predicted  
18 by the mathematical model properly described the experimental profiles. Regarding sulfide  
19 profiles, the simulated profiles accurately describe the experimental profiles from the  
20 beginning until the end of the biostat operation. The  $\text{S}^0$  profiles presented major deviations  
21 from the experimental data as  $\text{S}^0$  was only determined by mass balance. Thus, the absence of  
22 a  $\text{S}^0$  measurement and the successive solids accumulation and washing in the reactor due to  
23 biomass stuck over walls and stirrer lead to significant noisy  $\text{S}^0$  concentrations along the  
24 experimental periods. Nitrogen species are represented in Figure 5B, the model shows a  
25 production of  $7 \text{ mg L}^{-1}$  of  $\text{N-NO}_3^-$  during the first 5 days that was not observed  
26 experimentally; nevertheless, the mathematical model is in agreement with the experimental  
27 data for the rest of the operational periods. Regarding AOB activity,  $\text{N}_2\text{O}$  was not included  
28 in the mathematical model because  $\text{N}_2\text{O}$  was not measured and its production was estimated  
29 to be 7% (w/w) based on N imbalance. About DO, the experimental and the model data show  
30 similar behaviors with minor differences (Fig. 5C).

31

1 Although no biomass concentration as Volatile Suspended Solids (VSS) could be measured  
2 due to the presence of elemental sulfur, the active fractions of SOB, AOB and NOB  
3 concentrations along the experimental periods were calculated with the model (Fig. 5D).  
4 Because of biosulfur interference in the VSS analysis, the initial biomass concentration was  
5 estimated by performing a simulation of the start-up period (days 0 to 4) using all the kinetic  
6 parameters taken from the literature (Table SI2 in Supporting Information). This alternative  
7 was decided in order to avoid that the initial dynamics of the dissolved species were affected  
8 by an excessive offset of the simulated initial biomass concentration with respect to the real  
9 ones. According to the simulation, the SOB achieved the highest concentration during days  
10 24 to 27 (129 mg L<sup>-1</sup>) when complete oxidation occurred. When elemental sulfur  
11 accumulated after day 28, SOB decreased down to 113 mg VSS L<sup>-1</sup> until day 41 because of  
12 the lower growth yield of SOB with sulfide,  
13  $Y_{X/S^2-}$ , compared to elemental sulfur,  $Y_{X/S^0}$  (Table SI2 in Supporting Information).  
14 Afterward, the SOB concentration further decreased down to 65 mg VSS L<sup>-1</sup> and after the  
15 sulfide load shock on day 42, SOB decreased to 45 mg VSS L<sup>-1</sup> remaining steady until the  
16 end of the experimental period when the maximum elemental sulfur production was reached.  
17 In the case of AOB, during the first 4 days the model described small increase in the  
18 concentration to 24 mg VSS L<sup>-1</sup> which is explained by the low ammonium load. A complete  
19 washout is observed after 30 days of operation. NOB did not show any growth as it was  
20 washed out at the HRT of this experiment.

21

22 The accuracy of the simulation was evaluated by a t-student test. The null hypothesis to run  
23 this test was that the experimental and model values were statistically similar, and the main  
24 results of the t-test are shown in Table SI8 of the Supporting Information. The t-values were  
25 in the range of the t-critical for sulfide, sulfate and nitrite which means that the null  
26 hypothesis cannot be rejected.

27

28 It is worth mentioning that more accurate calibration could have been performed if  
29 experimental VSS concentrations could have been determined. Moreover, for a deeper  
30 understanding of the biological sulfur formation, a routine method to measure not only S<sup>0</sup> but  
31 also other intermediate sulfur species like polysulfide are warranted to have a better

1 prediction of the S-species concentration along the process and to obtain more accurate  
2 results in the process modelling.

3  
4 Beyond the limitations of the modelling approach, the statistical results showed good a  
5 matching among modelled and experimental data. Thus, this model can be further exploited  
6 in several ways, from helping in the design of future experiments<sup>50</sup> to its application to  
7 estimate the performance of biological systems where nitrogen and sulfide are involved.<sup>51</sup>  
8 Besides, this model can be applied to biostat-type systems to predict system behavior under  
9 different operational conditions such as sulfide/ammonium load ratios or hydraulic retention  
10 times. In addition, optimization of the oxygen supply as one of the most energy consuming  
11 operations in full-scale plants can be explored to, concomitantly, ensure the selectivity  
12 towards biosulfur formation. Similarly, the model could be used to predict the performance  
13 of AOB-enriched cultures as well as AOB cultures less sensitive to DO to explore the  
14 potential simultaneous, complete conversion of ammonium and sulfide to nitrite and  
15 biosulfur, respectively.

#### 16 17 *3.4 Assessment of the biosulfur production efficiency*

18 Biosulfur can be used in different processes as raw material. In the energy field, as a novel  
19 alternative of fossil fuels, Selvaraj *et al.*<sup>10</sup> was able to produce cathodes for Li-S batteries  
20 using sulfur produced biologically and able to recover 70% of it in these cathodes. In the  
21 agricultural sector, direct application of biosulfur as fertilizer has shown better efficiency  
22 than conventional sulfur.<sup>9</sup> Interestingly, since chemical sulfur is one of the main raw  
23 materials for S-based pigments such as methylene blue or ultramarine blue,<sup>12</sup> the use of  
24 biosulfur could also be evaluated as an alternative S-source for the synthesis of such  
25 pigments.

26 During the operational period with maximum sulfur production in the biostat (day 37 to the  
27 end of the experimental period) the solid phase composition was analyzed. Results showed  
28 that the dried solid contained a carbon, hydrogen, nitrogen and oxygen percentage (the main  
29 elements in biomass composition) of 25% (w/w) while elemental sulfur accounted for 75%  
30 (w/w). This was obtained at the end of the experimental period for a sulfide conversion to S<sup>0</sup>  
31 of 86% (w/w) at a sulfide loading rate of 25 mg S L<sup>-1</sup> d<sup>-1</sup>. It has been reported the use of



1 flocculants to enhance the sulfur precipitation. A 97.5% (w/w) efficiency in the sulfur  
2 recovery was found by Chen *et al.*<sup>52</sup> using polyaluminum chloride. Feng *et al.*<sup>53</sup> used an  
3 internal airlift loop reactor enriched with *halothiobacillus-type SOB* with flocculant-producer  
4 *Pseudomonas sp.* to enhance precipitation. A 96% (w/w) sulfur recovery efficiency was  
5 obtained. Despite flocculants can increase the sulfur recovery efficiency, they can affect  
6 sulfur purity and have a direct effect over the cost of the downstream process if biosulfur  
7 production as value-added product is targeted; Mora *et al.*<sup>11</sup> used a commercial flocculant  
8 (FL4820) for the effluent of a sulfur-producing biostat and obtained a 64.4% (w/w) and  
9 74.3% (w/w) of solid recovered and sulfur purity, respectively. Moreover, Janssen *et al.*<sup>54</sup>  
10 studied the aggregation of microbial sulfur production and found that by increasing the  
11 sulfide load, sulfur aggregation was enhanced without the addition of flocculants.  
12 Furthermore, the work presented herein demonstrates that treatment of ammonium and  
13 sulfide containing wastewater should be subjected to an additional N removal process if both  
14 N and biosulfur recovery are sought since both cannot be achieved simultaneously in a CSTR.

15

16

#### 17 **4. Conclusions**

18 Coupling of sulfide and ammonium biological oxidation in a biostat was studied to optimize  
19 biosulfur production at low HRT (25 h). The process showed that at a DO concentration of  
20 0.07 mg L<sup>-1</sup> and ORP of -380 ± 10 mV, 86% (w/) conversion of sulfide to S<sup>0</sup> with a purity of  
21 75% working with DO/S-TDS molar ratios of 0.44 was reached. AOB were not able to  
22 outcompete SOB under these conditions for the oxygen consumption, which was confirmed  
23 through a microbial diversity analysis. The mathematical model proposed to simulate the  
24 process described satisfactorily the experimental profiles. Overall, results obtained in the  
25 present study confirmed that ammonium and sulfide rich effluents could be fully valorized  
26 to produce optimally elemental sulfur, but further studies are warranted to evaluate the  
27 effectiveness of acclimatization periods to couple biological ammonium oxidation with  
28 biosulfur recovery. Moreover, the biosulfur produced presented low settleability indicating  
29 that further research should be performed to enhance its aggregation towards its valorization  
30 as a value-added product.

31

## 1 **5. Acknowledgments**

2 Authors are members of the GENOCOV research group from the Department of Chemical,  
3 Biological and Environmental Engineering at UAB (Universitat Autònoma de Barcelona).  
4 Authors acknowledge the Spanish Government, through the project RTI2018-099362-B-C21  
5 MINECO/FEDER, EU, for the financial support provided to perform this research.

## 7 **6. References**

- 8 1. Lens PNL, Visser A, Janssen AJH, Hulshoff Pol LW and Lettinga G. Biotechnological  
9 treatment of sulfate-rich wastewaters. *Crit. Rev. Environ. Sci. Technol.* 28(1): 41–88  
10 (1998).
- 11 2. Pokorna D and Zabranska J. Sulfur-oxidizing bacteria in environmental technology.  
12 *Biotechnol Adv.* 33(6): 1246–59 (2015).
- 13 3. Asadian M, Sabzi M and Anijdan SHM. The effect of temperature, CO<sub>2</sub>, H<sub>2</sub>S gases  
14 and the resultant iron carbonate and iron sulfide compounds on the sour corrosion  
15 behaviour of ASTM A-106 steel for pipeline transportation. *Int J Press Vessel Pip.*  
16 171: 184–93 (2019).
- 17 4. dos Santos JPL, de Carvalho Lima Lobato AK, Moraes C, de Lima Cunha A, da Silva  
18 GF and dos Santos LCL. Comparison of different processes for preventing deposition  
19 of elemental sulfur in natural gas pipelines: A review. *J Nat Gas Sci Eng.* 32: 364–72  
20 (2016).
- 21 5. Mannucci A, Munz G, Mori G and Lubello C. Anaerobic treatment of vegetable  
22 tannery wastewaters: A review. *Desalination* 264(1):1–8 (2010).
- 23 6. Fernández-Palacios E, Lafuente J, Mora M and Gabriel D. Exploring the performance  
24 limits of a sulfidogenic UASB during the long-term use of crude glycerol as electron  
25 donor. *Sci Total Environ.* 688: 1184–92 (2019).
- 26 7. Klimont Z, Smith SJ, Cofala J. The last decade of global anthropogenic sulfur dioxide:  
27 2000-2011 emissions. *Environ Res Lett.* 8:1 (2013).
- 28 8. Jones MT, Jerram DA, Svensen HH and Grove C. The effects of large igneous  
29 provinces on the global carbon and sulphur cycles. *Palaeogeogr Palaeoclimatol*  
30 *Palaeoecol.* 44(1): 4–21 (2016).
- 31 9. Lin S, Mackey HR, Hao T, Guo G, van Loosdrecht MCM and Chen G. Biological

- 1 sulfur oxidation in wastewater treatment: A review of emerging opportunities. *Water*  
2 *Res.* 143: 399–415 (2018).
- 3 10. Selvaraj H, Chandrasekaran K, Murugan R and Sundaram M. An integrated biological  
4 and electrochemical process for recovery of sulfur from an industrial effluent  
5 contaminated pond water and its preliminary application in high performance battery.  
6 *Sep Purif Technol.* 180: 133–41 (2017).
- 7 11. Mora M, Fernández-Palacios E, Guimerà X, Lafuente J, Gamisans X and Gabriel D.  
8 Feasibility of S-rich streams valorization through a two-step biosulfur production  
9 process. *Chemosphere.* 253: 1–10 (2020).
- 10 12. Škvarlová A, Kaňuchová M, Kozáková L, Valušová E, Holub M and Škvarla J.  
11 Preparation and characterization of ultramarine blue pigments from fly ash by using  
12 the X-ray photoelectron spectroscopy (XPS) for the determination of chemical states  
13 of sulphur in chromophores. *Microporous Mesoporous Mater.* 284: 283–8 (2019).
- 14 13. Sauvé S, Bernard S and Sloan P. Environmental sciences, sustainable development  
15 and circular economy: Alternative concepts for trans-disciplinary research. *Environ.*  
16 *Dev.* 17: 48–56 (2016).
- 17 14. Janssen a JH, Meijer S, Bontsema J and Lettinga G. Application of the Redox  
18 Potential for Controlling a Sulfideoxidizing Bioreactor. *Biotechnol Bioeng.* 60(2):  
19 147–55 (1998).
- 20 15. Heil J, Vereecken H and Brüggemann N. A review of chemical reactions of  
21 nitrification intermediates and their role in nitrogen cycling and nitrogen trace gas  
22 formation in soil. *European Journal of Soil Science.* 67(1): 23–39 (2016).
- 23 16. Guisasola A, Jubany I, Baeza JA, Carrera J and Lafuente J. Respirometric estimation  
24 of the oxygen affinity constants for biological ammonium and nitrite oxidation. *J*  
25 *Chem Technol Biotechnol.* 80(4): 388–96 (2005).
- 26 17. Perry RHG, Green DW and Maloney JO. *Perry's Chemical Engineers' Handbook* (7th  
27 Edition). McGraw-Hill. 1997.
- 28 18. Speight JG. *Industrial Inorganic Chemistry. Environmental Inorganic Chemistry for*  
29 *Engineers. Industrial Inorganic Chemistry for Engineers*, pp 111–169 (2017).
- 30 19. Nelson MI, Sidhu HS, Watt S and Hai FI. Performance analysis of the activated sludge  
31 model (number 1). *Food Bioprod Process.* 116: 41–53 (2019).

- 1 20. Wu J, He C, van Loosdrecht MCM and Pérez J. Selection of ammonium oxidizing  
2 bacteria (AOB) over nitrite oxidizing bacteria (NOB) based on conversion rates. *Chem*  
3 *Eng J.* 304: 953–61 (2016).
- 4 21. Roosta A, Jahanmiri A, Mowla D and Niazi A. Mathematical modeling of biological  
5 sulfide removal in a fed batch bioreactor. *Biochem Eng J.* 58: 50–6 (2011).
- 6 22. Mora M, López LR, Lafuente J, Pérez J, Kleerebezem R, van Loosdrecht MCM, et al.  
7 Respiriometric characterization of aerobic sulfide, thiosulfate and elemental sulfur  
8 oxidation by S-oxidizing biomass. *Water Res.* 89: 282–92(2016).
- 9 23. Hellinga C, Schellen AAJC, Mulder JW, Van Loosdrecht MCM and Heijnen JJ. The  
10 SHARON process: An innovative method for nitrogen removal from ammonium-rich  
11 waste water. *Water Sic. Technol.* 37(9): 135–42 (1998).
- 12 24. Tribe LA, Briens CL and Margaritis A. Determination of the volumetric mass transfer  
13 coefficient (kLa) using the dynamic “gas out–gas in” method: Analysis of errors  
14 caused by dissolved oxygen probes. *Biotechnol and Bioeng.* 46(4): 388–92 (1995).
- 15 25. He Z, Petiraksakul A and Meesapya W. Oxygen-Transfer Measurement in Clean  
16 Water. *J KMITNB.* 13(1): 14–9 (2003).
- 17 26. Reino C, Suárez-Ojeda ME, Pérez J and Carrera J. Kinetic and microbiological  
18 characterization of aerobic granules performing partial nitrification of a low-strength  
19 wastewater at 10 °C. *Water Res.* 101: 147–56 (2016).
- 20 27. Wichern M, Gehring T and Lübken M. Modeling of Biological Systems. *Treatise on*  
21 *Water Science.* Elsevier, pp 231– 263 (2011).
- 22 28. Yang Z, Fang KT and Kotz S. On the Student’s t-distribution and the t-statistic. *J*  
23 *Multivar Anal.* 98(6): 1293–304 (2007).
- 24 29. Lohwacharin J and Annachhatre AP. Biological sulfide oxidation in an airlift  
25 bioreactor. *Bioresour Technol.* 101: 2114–20 (2010).
- 26 30. Montebello AM, Mora M, López LR, Bezerra T, Gamisans X, Lafuente J, et al.  
27 Aerobic desulfurization of biogas by acidic biotrickling filtration in a randomly  
28 packed reactor. *J Hazard Mater.* 280: 200–8 (2014).
- 29 31. Klok JBM, de Graaff M, van den Bosch PLF, Boelee NC, Keesman KJ and Janssen  
30 AJH. A physiologically based kinetic model for bacterial sulfide oxidation. *Water Res.*  
31 47(2): 483–92 (2013).

- 1 32. Van Den Bosch PLF, Van Beusekom OC, Buisman CJN and Janssen AJH. Sulfide  
2 oxidation at halo-alkaline conditions in a fed-batch bioreactor. *Biotechnol Bioeng.*  
3 97(5): 1053–63 (2007).
- 4 33. Janssen AJH, Sleyster R, van der Kaa C, Jochemsen A, Bontsema J and Lettinga G.  
5 Biological sulphide oxidation in a fed-batch reactor. *Biotechnol Bioeng.* 47(3): 327–  
6 33 (1995).
- 7 34. Vassilev S V., Baxter D, Andersen LK and Vassileva CG. An overview of the  
8 chemical composition of biomass. *Fuel.* 89(5): 913–33 (2010).
- 9 35. Blázquez E, Bezerra T, Lafuente J and Gabriel D. Performance, limitations and  
10 microbial diversity of a biotrickling filter for the treatment of high loads of ammonia.  
11 *Chem Eng J.* 311: 91–9 (2017).
- 12 36. Maia GDN, Day V GB, Gates RS and Taraba JL. Ammonia biofiltration and nitrous  
13 oxide generation during the start-up of gas-phase compost biofilters. *Atmos Environ.*  
14 46: 659–64 (2012).
- 15 37. Bejarano Ortiz DI, Thalasso F, Cuervo López F de M and Texier AC. Inhibitory effect  
16 of sulfide on the nitrifying respiratory process. *J Chem Technol Biotechnol.* 88(7):  
17 1344–49 (2013).
- 18 38. Sekine M, Akizuki S, Kishi M and Toda T. Stable nitrification under sulfide supply in  
19 a sequencing batch reactor with a long fill period. *J Water Process Eng.* 25: 190– 94  
20 (2018).
- 21 39. Sekine M, Akizuki S, Kishi M, Kurosawa N and Toda T. Simultaneous biological  
22 nitrification and desulfurization treatment of ammonium and sulfide-rich wastewater:  
23 Effectiveness of a sequential batch operation. *Chemosphere* 244: 125381 (2020).
- 24 40. Jiang X, Luo Y, Yan R and Tay JH. Impact of substrates acclimation strategy on  
25 simultaneous biodegradation of hydrogen sulfide and ammonia. *Bioresour Technol.*  
26 100(23): 5707– 13 (2009).
- 27 41. Krishnakumar B, Majumdar S, Manilal VB and Haridas A. Treatment of sulphide  
28 containing wastewater with sulphur recovery in a novel reverse fluidized loop reactor  
29 (RFLR). *Water Res.* 39(4): 639–47(2005).
- 30 42. Vannini C, Munz G, Mori G, Lubello C, Verni F and Petroni G. Sulphide oxidation to  
31 elemental sulphur in a membrane bioreactor: Performance and characterization of the

- 1 selected microbial sulphur-oxidizing community. *Syst Appl Microbiol.* 31(6–8): 461–  
2 73 (2008).
- 3 43. Huber B, Herzog B, Drewes JE, Koch K and Müller E. Characterization of sulfur  
4 oxidizing bacteria related to biogenic sulfuric acid corrosion in sludge digesters. *BMC*  
5 *Microbiol.* 16(1): 1–11 (2016).
- 6 44. Lee CS, Kim KK, Aslam Z and Lee ST. *Rhodanobacter thiooxydans* sp. nov., isolated  
7 from a biofilm on sulfur particles used in an autotrophic denitrification process. *Int J*  
8 *Syst Evol Microbiol.* 57(8): 1775–9 (2007).
- 9 45. Munz G, Gori R, Mori G and Lubello C. Monitoring biological sulphide oxidation  
10 processes using combined respirometric and titrimetric techniques. *Chemosphere.*  
11 76(5): 644–50 (2009).
- 12 46. Jubany I, Lafuente J, Baeza JA and Carrera J. Total and stable washout of nitrite  
13 oxidizing bacteria from a nitrifying continuous activated sludge system using  
14 automatic control based on Oxygen Uptake Rate measurements. *Water Res.* 43(11):  
15 2761–72 (2009).
- 16 47. Pan Y, Ni BJ, Liu Y and Guo J. Modeling of the interaction among aerobic  
17 ammonium-oxidizing archaea/bacteria and anaerobic ammonium-oxidizing bacteria.  
18 *Chem Eng Sci.* 150(2): 35–40 (2016).
- 19 48. Ge S, Wang S, Yang X, Qiu S, Li B and Peng Y. Detection of nitrifiers and evaluation  
20 of partial nitrification for wastewater treatment: A review. *Chemosphere* 140: 85–98  
21 (2014).
- 22 49. Regmi P, Miller MW, Holgate B, Bunce R, Park H, Chandran K, et al. Control of  
23 aeration, aerobic SRT and COD input for mainstream nitrification/denitrification. *Water*  
24 *Res.* 57: 162–71 (2014).
- 25 50. Simpson R and Sastry SK. *Chemical and Bioprocess Engineering. Chemical and*  
26 *Bioprocess Engineering.* Springer, pp 245–61 (2013).
- 27 51. Frunzo L, Esposito G, Pirozzi F and Lens P. Dynamic mathematical modeling of  
28 sulfate reducing gas-lift reactors. *Process Biochem.* 47(12): 2172–81 (2012).
- 29 52. Chen F, Yuan Y, Chen C, Zhao Y, Tan W, Huang C, et al. Investigation of colloidal  
30 biogenic sulfur flocculation: Optimization using response surface analysis. *J Environ*  
31 *Sci.* 42: 227–35 (2016).

- 1 53. Feng S, Lin X, Tong Y, Huang X and Yang H. Biodesulfurization of sulfide  
 2 wastewater for elemental sulfur recovery by isolated *Halothiobacillus neapolitanus* in  
 3 an internal airlift loop reactor. *Bioresour Technol.* 264: 244–52 (2018).
- 4 54. Janssen A, De Keizer A, Van Aelst A, Fokkink R, Yangling H and Lettinga G. Surface  
 5 characteristics and aggregation of microbiologically produced sulphur particles in  
 6 relation to the process conditions. *Colloids Surfaces B Biointerfaces.* 6(2): 115–29  
 7 (1996).

8  
 9  
 10  
 11  
 12  
 13  
 14 **Table 1.** Oxygen-sulfide (O<sub>2</sub>/TDS) and oxygen-ammonium (O<sub>2</sub>/N-NH<sub>4</sub><sup>+</sup>) molar ratios and  
 15 mass transfer coefficients (K<sub>L</sub>a) supplied for each of the period defined by the air flow rate  
 16 evaluated during the biostat operation.

| Period   | I   | II   | III   | IV    | V     | VI    | VII   |
|--|-----|------|-------|-------|-------|-------|-------|
| Air flow rate (L min <sup>-1</sup> )                       | 1   | 0.7  | 0.5   | 0.35  | 0.2   | 0.05  | 0     |
| Duration (days)  | 0-6 | 6-10 | 10-14 | 14-17 | 17-23 | 23-37 | 37-62 |
| k <sub>L</sub> a (h <sup>-1</sup> )                        | 22  | 18.6 | 14.6  | 12.2  | 9.1   | 5.5   | 1.8   |
| O <sub>2</sub> /TDS molar ratio                            | 6.6 | 6    | 5.1   | 4.5   | 2.9   | 1.5   | 0.44  |
| O <sub>2</sub> /N-NH <sub>4</sub> <sup>+</sup> molar ratio | 7.3 | 7.2  | 4.8   | 4.2   | 3.2   | 2     | 0.5   |

17  
 18 **Table 2.** Values of the four parameters calibrated by the mathematical model.

| Parameters                     | Units                                      | Value |
|--------------------------------|--|-------|
| μ <sub>max/SOB</sub>           | d <sup>-1</sup>                            | 10.1  |
| k <sub>S0</sub>                | mg <sup>2/3</sup> VSS mg <sup>-2/3</sup> S | 0.3   |
| μ <sub>max/AOB</sub>           | d <sup>-1</sup>                            | 1.75  |
| k <sub>O<sub>2</sub>/AOB</sub> | mg L <sup>-1</sup>                         | 1.5   |

19  
 20  
 21

1

**Table 3.** Kinetic parameters reported in the literature and determined at 25 °C.

|                                | $\mu_{\max/\text{SOB}} (d^{-1})$ | $k_{S^0}$    | $\mu_{\max/\text{AOB}} (d^{-1})$ | $k_{\text{O}_2/\text{AOB}} (mg L^{-1})$ |
|--------------------------------|----------------------------------|--------------|----------------------------------|---|
| Munz et al. <sup>45</sup>      | 7.4                              |              |                                  |   |
| Mora et al. <sup>22</sup>      | 9.84                             | 0.833 – 0.03 |                                  |   |
| Wu et al. <sup>20</sup>        |                                  |              | 1.45                             |   |
| Jubant et al. <sup>46</sup>    |                                  |              | 1.21                             |   |
| Pan et al. <sup>47</sup>       |                                  |              |                                  | 0.6*                                    |
| Ge et al. <sup>48</sup>        |                                  |              |                                  | 0.22 – 0.56                             |
| Guisasola et al. <sup>16</sup> |                                  |              |                                  | 0.74                                    |
| Regmi et al. <sup>49</sup>     |                                  |              |                                  | 1.16                                    |

2

\* This parameter was reported at 22°C.

3